

Experimental Observation of the Inverse Spin Hall Effect at Room Temperature

Baoli Liu,^{1,*} Junren Shi,^{1,2,*} Wenxin Wang,¹ Hongming Zhao,¹
Dafang Li,¹ Shoucheng Zhang,³ Qikun Xue,^{1,2} and Dongmin Chen^{1,2}

¹*Beijing National Laboratory for Condensed Matter Physics,
Institute of Physics, Chinese Academy of Sciences, Beijing 100080, China*

²*International Center for Quantum Structures, Chinese Academy of Sciences, Beijing 10080, China*

³*Department of Physics, Stanford University, Stanford, CA 94305, USA*

We observe the inverse spin Hall effect in a two-dimensional electron gas confined in AlGaAs/InGaAs quantum wells. Specifically, we find that an inhomogeneous spin density induced by the optical injection gives rise an electric current transverse to both the spin polarization and its gradient. The spin Hall conductivity can be inferred from such a measurement through the Einstein relation and the Onsager relation, and is found to have the order of magnitude of $0.5(e^2/h)$. The observation is made at the room temperature and in samples with macroscopic sizes, suggesting that the inverse spin Hall effect is a robust macroscopic transport phenomenon.

Electrically controlling spins has been a major theme for the recent studies of the spin electronics, promising future information processing devices integrating both the charge and spin operations [1, 2, 3]. As one of the most elementary transport processes involving both spins and charges, the spin Hall effect (SHE), i.e., the transverse spin transport induced by an electric field, is the focus of the recent theoretical studies [4, 5, 6, 7]. Experimentally, both the spin accumulation measurements [8, 9, 10] and the electronic measurement [11] have demonstrated the convincing evidence for the existence of SHE. Electrical measurement of the spin current has also been reported [12].

In this Letter, we experimentally investigate the reciprocal effect of SHE – the inverse spin Hall effect (ISHE), in semiconductors. ISHE complements the SHE, demonstrating the possibility of charge transport driven by the spin degrees of freedom. Because ISHE is closely related to SHE by the general principle of Onsager relation, which dictates the symmetry of the transport coefficients for the SHE and its reciprocal, our study also provides a supplemental evidence for the existence of SHE. Moreover, it also provides an accessible way to quantitatively determine the spin Hall conductivity of a sample.

It is instructive to have a general theoretical analysis for the relevant phenomena. For an isotropic two-dimensional (2D) system with the time-reversal symmetry (e.g., non-magnetic systems), the set of the equations describing the macroscopic near-equilibrium (lin-

ear) charge and spin transports can be written as,

$$\begin{aligned} \mathbf{j}_{\text{tr}}^c &= -qD^{cc}\nabla\left[n(\mathbf{x}) + \left(\frac{\partial n}{\partial\mu}\right)_h q\phi(\mathbf{x})\right] \\ &\quad - qD_H^{cs}\hat{\mathbf{z}} \times \nabla\left[S_z(\mathbf{x}) - \left(\frac{\partial S_z}{\partial h_z}\right)_\mu h_z(\mathbf{x})\right], \\ \mathbf{j}_{\text{tr}}^s &= -D^{ss}\nabla\left[S_z(\mathbf{x}) - \left(\frac{\partial S_z}{\partial h_z}\right)_\mu h_z(\mathbf{x})\right] \\ &\quad - D_H^{sc}\hat{\mathbf{z}} \times \nabla\left[n(\mathbf{x}) + \left(\frac{\partial n}{\partial\mu}\right)_h q\phi(\mathbf{x})\right], \end{aligned} \quad (1)$$

where \mathbf{j}_{tr}^c (\mathbf{j}_{tr}^s) denotes the charge (spin) transport current, and $n(\mathbf{x})$ ($S_z(\mathbf{x})$) is the local number (spin) density of the carriers, respectively. q is the charge of the carrier; $\hat{\mathbf{z}}$ is the unit vector perpendicular to the 2D conducting plane, and the transport (diffusion) coefficients are denoted by D with the appropriate superscripts and subscripts (s denotes spin, c denotes charge, H denotes the transverse Hall transport). The external fields are imposed by the electric potential $\phi(\mathbf{x})$ and the Zeeman field $h_z(\mathbf{x})$. For simplicity and without loss the generality, only the transport induced by the z -component of the spin density is considered. The validity of Eq. (1) can be established through the general considerations of symmetries, as well as the constraint that the transport currents must vanish when the (spin) density distribution is in the equilibrium against the external fields (i.e., $n(\mathbf{x}) = n_0 - (\partial n/\partial\mu)_h q\phi(\mathbf{x})$ and $S_z(\mathbf{x}) = S_z^0 + (\partial S_z/\partial h_z)_\mu h_z$).

Equation (1) fully describes the near-equilibrium charge and spin transport, for both the diffusion induced by the (spin) density inhomogeneity and the transport induced by the external fields. Within this framework, the inverse spin Hall effect is described by $\mathbf{j}_{\text{tr},H}^c = \sigma^{\text{ISH}}\hat{\mathbf{z}} \times \mathbf{F}_s$ with the spin force being defined as the gradient of Zeeman field $\mathbf{F}_s = g\mu_B\nabla h_z(\mathbf{x})$ [13, 14]. It can be related to the transverse charge diffusion induced by the spin density inhomogeneity:

$$\mathbf{j}_{\text{tr},H}^c = -qD_H^{cs}\hat{\mathbf{z}} \times \nabla S_z(\mathbf{x}) \quad (2)$$

via an Einstein relation that relates the inverse spin Hall conductivity σ^{ISH} with the corresponding diffusion constant D_H^{cs} :

$$\sigma^{\text{ISH}} = (q/g\mu_B)(\partial S_z/\partial h_z)_\mu D_H^{cs}. \quad (3)$$

Moreover, the Onsager relation dictates the duality between ISHE and SHE [14]:

$$\sigma^{\text{SH}} = \sigma^{\text{ISH}}, \quad (4)$$

where σ^{SH} is the spin Hall conductivity ($\mathbf{j}_{\text{tr}, H}^s = \sigma^{\text{SH}} \hat{\mathbf{z}} \times \mathbf{E}$).

Equations (2)–(4) outline the general theoretical ground for our experimental scheme: if we can observe and experimentally establish the ISHE diffusion process described by Eq. (2), then the ISHE and SHE can be related to such a measurement by the Einstein relation (3) and the Onsager relation (4). We stress that the theoretical ground of our experimental scheme is the direct result of the general principles of the non-equilibrium thermodynamics, and should be valid for any macroscopic near-equilibrium transport phenomena, regardless the microscopic details of the system. On the other hand, building a microscopic transport theory consistent to these general principles is a nontrivial issue yet to be fully clarified [14].

The experimental setup for observing the ISHE diffusion process is shown schematically in Fig. 1(a). A circularly polarized laser light spot is employed to create an inhomogeneous spin density with Gaussian spatial profile [15]. An overall gradient of spin density along x -direction is naturally generated when the light spot is cutoff by the edges of the 2DEG channel, resulting in asymmetric distribution of spin density. The electric current due to the ISHE can then be measured along y -direction. In such a setup, the transverse electric current is maximized when the the light spot is centering at an edge of the channel, and reverses its direction when centering at the opposite edge. The current vanishes when the light spot is moved to the center of the channel, as the spatial distribution of spin density is symmetric in this case. This characteristic behavior of ISHE can be revealed by scanning the light spot along x -direction to observe the dependence of the electric current on the position of light spot. In theory, we find that total transverse electric current is:

$$I_y = -q\gamma D_H^{cs} \overline{\Delta S_z}, \quad (5)$$

where $\overline{\Delta S_z} = (1/L) \int_0^L dy \Delta S_z(y)$ is the overall gradient of the spin density along x -direction, averaged over the y -direction of the channel. $\Delta S_z(y) \equiv S_z(x = \text{right edge}, y) - S_z(x = \text{left edge}, y)$ is the difference of spin density at the right and the left edges of the channel for given y , L is the length of the sample, and $\gamma = R_c/(R_c + R_I)$ with R_c and R_I being the resistance of the 2DEG channel and the measurement circuit, respectively [19].

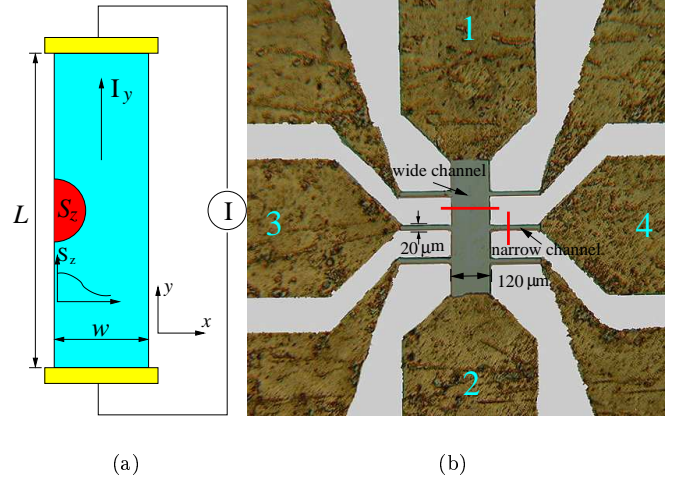


Figure 1: (a) The schematics of the experimental setup: an inhomogeneous spin density with Gaussian spatial profile is created in a 2DEG channel using a circularly polarized light spot with normal incidence. The transverse electric current induced by ISHE is measured in the y -direction. (b) The lithography image of the device: a multi-terminal Hall bar (indicated by the gray region) with a $400\mu\text{m} \times 120\mu\text{m}$ main channel and six $150\mu\text{m} \times 20\mu\text{m}$ arms, from which we obtain one wide measurement channel by utilizing the main channel of the Hall bar ($w = 120\mu\text{m}$, $L = 400\mu\text{m}$), and three narrow measurement channels formed from three pairs of the arms ($w = 20\mu\text{m}$, $L = 300\mu\text{m}$), as indicated in the image. The red lines indicate the scanning paths of the light spot for obtaining the results presented in Fig. 2, and the electric current is measured through the electrodes 1 – 2 for the wide channel, and the electrodes 3 – 4 for the narrow channel, respectively.

The sample is grown by molecular beam epitaxy (MBE) on the semi-insulating (001) GaAs substrate. 20 periods GaAs(2nm)/AlGaAs(6nm) superlattices are first grown on the substrate, followed by 15nm $\text{Al}_{0.24}\text{Ga}_{0.76}\text{As}$. 2DEG formed in a 13nm $\text{In}_{0.19}\text{Ga}_{0.81}\text{As}$ quantum well, which is sandwiched between the barriers of 30nm GaAs and 39nm $\text{Al}_{0.24}\text{Ga}_{0.76}\text{As}$. Si δ -doping layers are buried in GaAs and $\text{Al}_{0.24}\text{Ga}_{0.76}\text{As}$ barriers with 10nm and 4nm spacer layers, respectively. The standard Hall measurement gives the electron concentration $n = 4.2 \times 10^{12}\text{cm}^{-2}$ and the mobility $\mu = 5000\text{cm}^2/\text{V} \cdot \text{s}$ at the room temperature. Multi-terminal device of Hall bar geometry is patterned using the standard photolithography and wet etching, and the ohmic contacts are made with annealed AuGe/Ni. By utilizing the main channel of the Hall bar and its six arms, we obtain one wide channel and three narrow channels suitable for the proposed experiments, as shown in Fig. 1(b). All the measurements are performed at the room temperature. Another sample with the same geometry is also prepared on (110) GaAs substrate. Both samples yield the similar results, and only the results for the (001) sample will be

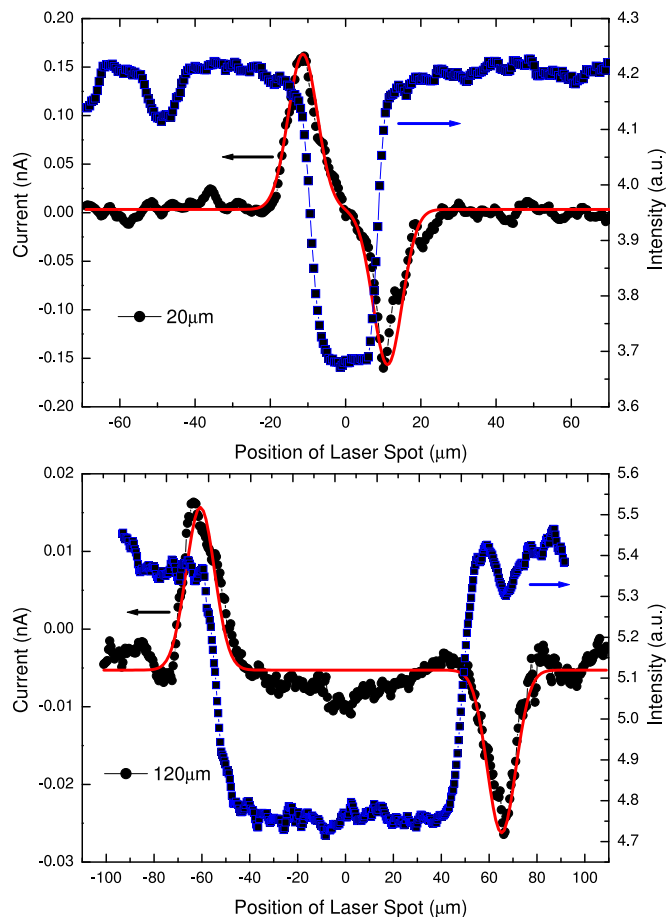


Figure 2: The light-spot-position dependence of the ISHE current induced by a circularly polarized light, shown as black dots. The blue-square curve shows the the intensity of reflected light: the region occupied by the channel has the lower reflectivity due to the additional absorption of light by the 2DEG. It thus provides a direct sectional profile of the 2DEG channel along the scanning path, as well as the precise determination of the position of the light spot relative to the channel. Red curve shows the theoretical fitting to the line-shape of electric current with the form described in the text. The results for both a narrow channel (upper panel) and a wide channel (lower panel) are shown.

presented in the following.

In the experiment, a tunable continuous-wave Ti-Sapphire laser is employed for the inter-band excitation with 20mW average pump power at the wavelength of 830nm. Its polarization is modulated by a photo-elastic modulator (PEM), which yields a periodically oscillating polarization between right- (σ^+) and left- (σ^-) circularly polarized light with a period of 50kHz and a constant light intensity, resulting in a modulated spin density and a constant carrier density [16]. The laser light is focused to spot with full-width at half maximum (FWHM) of $8.0\mu\text{m}$ through an objective (N.A. = 0.38), and is normal to the sample. The spatial distribution of the z -component spin density had been independently

measured by the time and spatially resolved Kerr rotation spectroscopy in such system, and was found to have the Gaussian profile. The sample position is precisely controlled by a motorized translation stage with $0.1\mu\text{m}$ unidirectional repeatability (Physik Instrumente, M-126.DG). By moving the sample, the center of the light spot is scanned across the channel. The position of the light spot on the sample is precisely determined through the simultaneous measurement of the intensity of reflected light from the sample surface, which provides a direct profiling of sectional geometry of the channels along the scanning paths. The electric current is measured directly by the lock-in amplifier, which effectively filters out the electric current induced by effects not related to spins such as the Dember effect and the photovoltaic effects, as the PEM only modulates the spin density but keeps the carrier density constant.

Figure 2 presents the main results of this study. For both the wide and the narrow channels, the light-spot-position dependence of the electric current shows the characteristic N -shape: it peaks at the two edges with the opposite signs, and vanishes at the center of the channel. The same behavior is observed in other scanning paths and channels as well. The behavior is consistent with what the theory expects from the ISHE diffusion process, Eq. (2). For a more quantitative analysis, we notice that the spin diffusion length of the sample $\sim 1\mu\text{m}$ is much smaller than the size of the light spot, thus the spin density $S_z(\mathbf{x})$ excited by the circularly polarized light can be considered to be proportional to the local light intensity: $S_z(\mathbf{x}) \propto I(\mathbf{x})$. The intensity profile of a laser light spot is well described by the Gaussian shape $I(\mathbf{x}) = I_0 \exp[-(\mathbf{x} - \mathbf{x}_0)^2/2\sigma^2]$, where σ is related to the FWHM of the laser spot by $\sigma = \text{FWHM}/2\sqrt{2\ln 2} \approx 3.4\mu\text{m}$. The ISHE current has the form $I_y \propto \Delta S_z \propto \exp[-x_0^2/2\sigma^2] \sinh(x_0 w/2\sigma^2)$, where x_0 is the center position of the light spot, and w is the width of the channel. The form fits the line-shape of the experimental data well. For the narrow channel, the fitting yields $w = 22.5 \pm 0.2\mu\text{m}$ and $\sigma = 3.9 \pm 0.1\mu\text{m}$, consistent with the independently determined values $w = 21\mu\text{m}$ (determined from the intensity of reflected light, blue square curves in Fig. 2) and $\sigma = 3.4\mu\text{m}$. For the wide channel, it yields $w = 125.8 \pm 0.3\mu\text{m}$ (vs. the independently determined value $w = 123\mu\text{m}$) and $\sigma = 6.2 \pm 0.2\mu\text{m}$, and the somewhat over-estimated σ is due to the less sharp boundary of the edges (see the blue square curve in the bottom panel of Fig. 2). The good correspondence between the experiment and the theory provides a strong evidence for the existence of the ISHE.

While the observation can be naturally associated with the ISHE diffusion process, it is necessary to rule out other possibilities that may give rise the same behavior. We present the following points in order: (i) the fact that the same behavior is observed in a number of different channels and in a couple of different samples rules

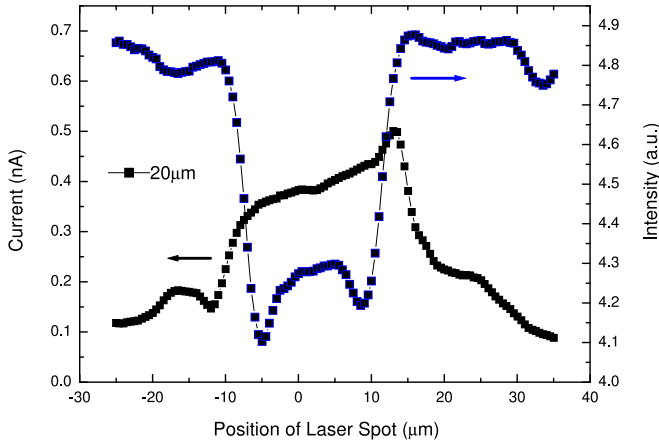


Figure 3: The electric current measured with the linearly polarized light (black dots). The electric current measurement is locked-in to the modulation of the light intensity (carrier density). The blue squares indicate the intensity of reflected light.

out the possibility that it is caused by the asymmetry or inhomogeneity of the channels; (ii) the fact that the electric current has the opposite signs at the opposite edges of the channel indicates that the transport must be driven by the gradient of the non-equilibrium density (either charge or spin). This rules out the transport mechanisms that are driven by the non-equilibrium density itself, for instance, the circular photo-galvanic effect [17, 18], for which the electric current is induced by the spin density, and flows along a fixed direction resulted from the reduced symmetry of the sample; (iii) the circularly polarized light employed in the measurement excites the charge density as well as the spin density. This rises the possibility that the phenomenon is induced by the gradient of the charge density instead of the spin density, i.e., the modulation of the circular polarization may induce a modulation of the charge density, which in turn generates an electric signal picked up by the lock-in amplifier. While this is highly improbable in theory because the sample has the time-reversal symmetry which prohibits the charge Hall transport, the possibility can be explicitly ruled out by a controlled experiment: in Fig. 3, the linearly polarized light is employed to excite a pure charge density. It is evident that the incriminating N -shape characteristics seen in the circularly polarized light measurement (Fig. 2) can no longer be observed. All summarized, we conclude that the electric current measured in Fig. 2 can only be induced by the gradient of spin density, as predicted by Eq. (2).

Finally, we can quantitatively determine the (inverse) spin Hall conductivity based on such a measurement. For 20mW light power, the total injection rate (I.R.) of spins is estimated to be 3.9×10^{14} spins/s [20]. The total number of the injected spins $S_{\text{tot}} = \text{I.R.} \times \tau_s \approx 3.9 \times 10^4$ spins with a spin relaxation time $\tau_s \approx 100$ ps. By using

Eq. (5), the magnitude of the ISHE diffusion constant can be estimated by $D_H^{cs} \approx \sqrt{2\pi} I_y^{\text{max}} \sigma L / (\epsilon \gamma S_{\text{tot}})$ (assuming $w \gg \sigma$), and yields values $D_H^{cs}(20\mu\text{m}) \approx 0.87\text{cm}^2/\text{s}$ and $D_H^{cs}(120\mu\text{m}) \approx 0.4\text{cm}^2/\text{s}$, respectively [21]. By applying the Einstein relation Eq. (3), $\sigma^{\text{SH}} \approx (ne/kT)D_H^{cs}$ ($\partial S_z / \partial h_z \approx g\mu_B n/kT$), we get the spin Hall conductivity (in the unit of charge conductivity): $\sigma^{\text{SH}}(20\mu\text{m}) \approx 0.59(e^2/h)$ and $\sigma^{\text{SH}}(120\mu\text{m}) \approx 0.27(e^2/h)$, respectively. The spin Hall conductivities determined from the two different channels yield consistent values (within a factor of 2), indicating the self-consistency of our method of analysis. We note that all the parameters involved in the estimate can in principles be precisely determined. Our experimental scheme can thus provide an accessible way to measure the spin Hall conductivity.

In summary, we have observed the ISHE diffusion process, experimentally establishing one of the elementary processes of the spin-charge transports. Because ISHE is closely related to SHE by the general principle of Onsager relations, the observation provides a supplemental evidence for the existence of the spin Hall effect. Moreover, our experimental scheme provides an accessible way to quantitatively determine the spin Hall conductivity of the system, implying the wider application of the technique in the future studies of the spin-charge transports. Finally, the fact that the measurement is carried out at the room temperature and in samples with macroscopic sizes suggests that ISHE is a robust macroscopic transport phenomenon – a universal property that presents in various systems.

We gracefully acknowledge the useful discussions with Qian Niu and Yugui Yao, and the assistance of Changzhi Gu for preparing the devices. This work was supported by the Knowledge Innovation Project of the Chinese Academy of Sciences, and NSFC-10534030. J.R.S. was supported by the ‘‘BaiRen’’ program of the Chinese Academy of Sciences.

* These authors contribute equally to this work.

- [1] G. A. Prinz, *Science* **282**, 1660 (1998).
- [2] S. A. Wolf, *et al.*, *Science* **294**, 1488 (2001).
- [3] I. Zutic, J. Fabian, S. D. Sarma, *Rev. Mod. Phys.* **76**, 323 (2004).
- [4] M. I. Dyakonov, V. I. Perel, *Phys. Lett. A* **35**, 459 (1971).
- [5] J. E. Hirsch, *Phys. Rev. Lett.* **83**, 1834 (1999).
- [6] S. Murakami, N. Nagaosa, S.-C. Zhang, *Science* **301**, 1348 (2003).
- [7] J. Sinova, *et al.*, *Phys. Rev. Lett.* **92**, 126603 (2004).
- [8] Y. K. Kato, R. C. Myers, A. C. Gossard, D. D. Awschalom, *Science* **306**, 1910 (2004).
- [9] J. Wunderlich, B. Kaestner, J. Sinova, T. Jungwirth, *Phys. Rev. Lett.* **94**, 047204 (2005).
- [10] H. Zhao, E. J. Loren, H. M. van Driel, A. L. Smirl, *Phys. Rev. Lett.* **96**, 246601 (2006).
- [11] S. O. Valenzuela, M. Tinkham, *Nature* **442**, 176 (2006).

- [12] X.-D. Cui, S.-Q. Shen, J. Li, W. Ge, F.-C. Zhang, *preprint* pp. cond-mat/0608546 (2006).
- [13] P. Zhang, Q. Niu, *Preprint* pp. cond-mat/0406436 (2004).
- [14] J. Shi, P. Zhang, D. Xiao, Q. Niu, *Phys. Rev. Lett.* **96**, 076604 (2006).
- [15] F. Meier, B. P. Zakharchenya, eds., *Optical Orientation* (Elsevier, Amsterdam, 1984).
- [16] B. Koopmans, J. E. M. Haverkort, W. J. M. de Jonge, G. Karczewski, *J. Appl. Phys.* **85**, 6763 (1999).
- [17] S. D. Ganichev, *et al.*, *Phys. Rev. Lett.* **86**, 4358 (2001).
- [18] S. D. Ganichev, H. Ketterl, W. Prettl, E. L. Ivchenko, L. E. Vorobjev, *Appl. Phys. Lett.* **77**, 3146 (2000).
- [19] Equation (5) is a direct result of the more general formula
- $$I_y = -q \oint dy \rho_c(y) D_H^{cs} \Delta S_z(y) / \oint dy \rho_c(y),$$
- where $\rho_c(y)$ is the resistivity, and the integration is over the closed loop of the circuit.
- [20] I.R. = $(1/2)P/(h\nu)(T\alpha d)$, where $h\nu \approx 1.5\text{eV}$, $T \approx 0.6$ is the transmission rate of the light path, $\alpha d = 4\pi kd/\lambda \approx 0.016$ is the absorption rate of the 2DEG ($k = 0.08$, $d = 13\text{nm}$ is the thickness of the quantum well). The extra factor of $1/2$ is due to the fact that both the heavy hole and the light hole states are excited.
- [21] The parameters used: for $20\mu\text{m}$ channel: $R_c = 6.2\text{k}\Omega$, $I_y^{\text{max}} = 0.16\text{nA}$, $L = 300\mu\text{m}$; for $120\mu\text{m}$ channel: $R_c = 1.1\text{k}\Omega$, $I_y^{\text{max}} = 0.021\text{nA}$, $L = 400\mu\text{m}$. The measurement circuit has an inner resistance $R_I = 1\text{k}\Omega$.